

UHI Research Database pdf download summary

Concept for a hyperspectral remote sensing algorithm for floating marine macro plastics

Goddijn-Murphy, Lonneke; Peters, Steef; van Sebille, Erik; James, Neil; Gibb, Stuart

Published in:
Marine Pollution Bulletin

Publication date:
2018

Publisher rights:
© 2017 Elsevier Ltd.

The re-use license for this item is:
CC BY-NC-ND

The Document Version you have downloaded here is:
Peer reviewed version

The final published version is available direct from the publisher website at:
[10.1016/j.marpolbul.2017.11.011](https://doi.org/10.1016/j.marpolbul.2017.11.011)

[Link to author version on UHI Research Database](#)

Citation for published version (APA):

Goddijn-Murphy, L., Peters, S., van Sebille, E., James, N., & Gibb, S. (2018). Concept for a hyperspectral remote sensing algorithm for floating marine macro plastics. *Marine Pollution Bulletin*, 126, 255–262. DOI: 10.1016/j.marpolbul.2017.11.011

General rights

Copyright and moral rights for the publications made accessible in the UHI Research Database are retained by the authors and/or other copyright owners and it is a condition of accessing publications that users recognise and abide by the legal requirements associated with these rights:

- 1) Users may download and print one copy of any publication from the UHI Research Database for the purpose of private study or research.
- 2) You may not further distribute the material or use it for any profit-making activity or commercial gain
- 3) You may freely distribute the URL identifying the publication in the UHI Research Database

Take down policy

If you believe that this document breaches copyright please contact us at RO@uhi.ac.uk providing details; we will remove access to the work immediately and investigate your claim.

1 **Title:** Concept for a hyperspectral remote sensing algorithm for floating marine macro plastics

2

3 **Contributing authors:**

4

5 Lonneke Goddijn-Murphy (lead author)

6 Environmental Research Institute, UHI-NHC, Thurso, Scotland, UK

7

8 Steef Peters

9 Water Insight BV, Wageningen, The Netherlands

10

11 Erik van Sebille

12 1) Institute for Marine and Atmospheric research, Utrecht University, Utrecht, Netherlands

13 2) Grantham Institute, Imperial College London, London, United Kingdom

14

15 Neil A. James

16 Environmental Research Institute, UHI-NHC, Thurso, Scotland, UK

17

18 Stuart Gibb

19 Environmental Research Institute, UHI-NHC, Thurso, Scotland, UK

20

21

22 **Corresponding author:**

23 Lonneke Goddijn-Murphy

24 Environmental Research Institute

25 CfEE Building, UHI-NHC

26 Ormlie Road, Thurso, KW14 7EE

27 Scotland

28 +44(0)1847 889664

29 Lonneke.Goddijn-Murphy@uhi.ac.uk

30

1 **ABSTRACT**

2 *There is growing global concern over the chemical, biological and ecological impact of plastics in the*
3 *ocean. Remote sensing has the potential to provide long-term, global monitoring but for marine*
4 *plastics it is still in its early stages. Some progress has been made in hyperspectral remote sensing of*
5 *marine macroplastics in the visible (VIS) to short wave infrared (SWIR) spectrum. We present a*
6 *reflectance model of sunlight interacting with a sea surface littered with macro plastics, based on*
7 *geometrical optics and the spectral signatures of plastic and seawater. This is a first step towards the*
8 *development of a remote sensing algorithm for marine plastic using light reflectance measurements*
9 *in air. Our model takes the colour, transparency, reflectivity and shape of plastic litter into account.*
10 *This concept model can aid the design of laboratory, field and Earth observation measurements in*
11 *the VIS-SWIR spectrum and explain the results.*

12 **KEYWORDS:** Plastic debris; Remote Sensing; Marine environment; Pollution

1 **1 BACKGROUND**

2 Marine plastic litter is a global environmental problem that is of increasing concern (Rochman *et al.*, 2016). Global plastic production increases annually (Andrady & Neal, 2009), with an estimated
3 *al.*, 2016). Global plastic production increases annually (Andrady & Neal, 2009), with an estimated
4 4.8 to 12.7 million metric tons of plastic entering the oceans each year (Jambeck *et al.*, 2015),
5 posing a threat to seabirds (Wilcox *et al.*, 2015), fish (Gregory, 2009), turtles (Mrosovsky *et al.*,
6 2009) and marine mammals (Laist, 1997). However, there are still many questions about its
7 sources, sinks, pathways, and trends in abundance of marine plastic litter, its harmful impacts on
8 human and marine life, and the effectiveness of potential clean-up operations. Some surveys have
9 been undertaken (e.g., Eriksen *et al.*, 2014) but there is a lack of long-term, large scale monitoring.
10 Remote sensing (RS) has the potential to provide long-term, global monitoring of floating marine
11 plastics but is still in its infancy (Maximenko, 2016). In this paper, we describe a concept RS method
12 for marine plastic litter floating on top of the sea surface, based on geometrical optics and the
13 spectral signatures of plastic and seawater. The objective is to find a method that can derive the
14 surface fraction of plastic floating on the sea surface from the measured reflectance of natural
15 daylight in air. Asner (2016) has made some progress in the remote sensing of marine
16 macroplastics in the visible (VIS) to short wave infrared (SWIR) spectrum and we base our
17 modelling and experimental work on their reflectance spectra. VIS ranges from 400-780 nm, SWIR
18 from 1.1 to 3 μm , and NIR (near infrared) represents the wavelengths in between.

19 Addressing questions around marine plastic litter is complicated because many different types of
20 plastic exist in the marine environment. Plastic size can range from microplastics (smaller than 5
21 mm) to large plastic pieces such as “ghost nets” (lost or discarded fishing nets). The former can be
22 toxic through adsorption of pollutants onto plastics and ingested by marine life and the latter can

1 entangle animals and endanger mariners. Microplastics can originate from pellets or “nurdles”
2 used in manufacturing, microbeads originate from certain cosmetic and personal care products,
3 and textile fibres that enter the ocean in wastewater (primary microplastics) and from
4 fragmentation of larger plastic pieces (secondary microplastics). According to Filella (2015) it is
5 likely that this secondary source of microplastics dominates, or will dominate, the microplastics
6 found in the marine environment. They base this expectation on the observation that the amount
7 of macroplastic accumulating in the marine environment is increasing, while primary microplastics
8 are predicted to decrease due to recent antipollution measurements. Therefore, by studying
9 macroplastics in the ocean, one of the major and increasingly more important sources of
10 microplastics are also studied. Unlike microplastics, larger plastics located using remote sensing
11 could potentially be removed from the sea and coastlines – contributing to the effort to “clean up”
12 the ocean (Sherman & van Sebille, 2016). Plastic comes in many different chemical compositions,
13 each with different properties and buoyancy. Common marine plastic polymers include
14 polyethylene (PE), polypropylene (PP), polyvinylchloride (PVC), polystyrene (PS), and polyamide
15 (nylons), whilst they may be in the form of pellets, beads, films, fragments, fibres/filaments, and
16 foamed plastic. Marine plastic litter persists in the environment for varying, and mostly very long,
17 times; it degrades under the influence of ultraviolet light of the sun and chemicals dissolved in
18 seawater and fragments in breaking waves and collisions. The contribution of micro-organisms to
19 the degradation of plastics in the marine environment by biological decomposition is negligible
20 (Andrady, 2015). However, according to Eriksen *et al.* (2014), bacterial degradation becomes more
21 important as plastic particles become smaller and facilitate their export from the sea surface in
22 addition to the ingestion of smaller plastic particles by organisms. Plastic objects in the ocean
23 attract marine life and all floating objects are biofouled. Biofouling will reduce the buoyancy of

1 plastic particles, so that they sink below the sea surface. Small plastic items start sinking sooner
2 than larger plastic items because buoyancy is related to item volume, whereas fouling is related to
3 surface area, and small items have high surface area to volume ratios (Ryan, 2015). In summary,
4 there is a wide range of sizes, types, shapes, and of chemical composition of plastic in the ocean.
5 We will focus on floating macroplastics because buoyant microplastics do not stay on top of the
6 ocean surface but are mostly in suspension and lost from the sea surface (Eriksen *et al.*, 2014).
7 Microplastics will therefore not be “seen” by our proposed method. Considering that marine
8 plastic RS is still in its early stages, we think this is a reasonable starting point.

9 This paper is organized as in the following. First, we briefly describe the much-studied reflectance
10 of sunlight of the open sea. Next, we investigate the consequences of introducing floating plastic
11 to the sea surface in a theoretical approach and propose a mathematical reflectance model to
12 calculate the changed reflectance. This model will necessarily be an approximation and in the
13 consequent section, we discuss the neglected terms. Finally, we suggest measurements to verify
14 the proposed model and give a short conclusion. The parameter definitions used in this paper are
15 listed in Table 1 and illustrated in Figs. 1-2.

16 **2 REFLECTANCE MODEL**

17 **2.1 *Light reflectance of natural waters***

18 As can be seen in Fig. 1a, downwelling sunlight hitting the water partly reflects directly at the water
19 surface and partly penetrates the surface refracting downwards. In the water body, light photons
20 are absorbed and scattered in all directions. Because of the repeated scattering, subsurface
21 upwelling light in water is generally considered to be Lambertian, i.e., light is evenly distributed in
22 all directions. If the water is optically deep (bottom is invisible), the fraction of light that scatters

1 *Table 1. Definitions of the variables used in this paper; subscript "0" indicates in the absence of*
 2 *plastic.*

<i>variable</i>	<i>definition</i>	<i>Unit</i>
A_p	Area covered by plastic, projected in nadir view	[m ²]
A_w	Total area projected in nadir view	[m ²]
ε	$L_{ds}/L_{ds,0}$	
f	plastic area fraction A_p/A_t	
F	Fraction diffuse sky ligh $E_{d,dif}/E_d$	
E_d	Downwelling irradiance in air	[wm ⁻²]
E_{ws}	Upwelling irradiance in water	[wm ⁻²]
L_d	Downwelling radiance in air	[wm ⁻² sr ⁻¹]
L_{ds}	Downwelling radiance in water	[wm ⁻² sr ⁻¹]
L_p	Total plastic leaving radiance in air ($L_{pr} + L_{pt}$)*	[wm ⁻² sr ⁻¹]
L_{pr}	L_d reflected by plastic in air*	[wm ⁻² sr ⁻¹]
L_{ps}	Total plastic leaving, downwelling radiance in water*	[wm ⁻² sr ⁻¹]
L_{pt}	L_{ws} transmitted upwards through plastic in air*	[wm ⁻² sr ⁻¹]
L_w	Total water leaving radiance in air ($L_{wr} + L_{wt}$)*	[wm ⁻² sr ⁻¹]
L_{wr}	L_d reflected by air-water interface*	[wm ⁻² sr ⁻¹]
L_{ws}	Sub surface upwelling radiance in water*	[wm ⁻² sr ⁻¹]
L_{wt}	L_{ws} transmitted through water-air interface*	[wm ⁻² sr ⁻¹]
L_t	Total upwelling radiance ($L_w + L_p$)*	[wm ⁻² sr ⁻¹]
R	Ratio of upwelling radiance in nadir view and E_d in air	[sr ⁻¹]
R_p	L_p/E_d	[sr ⁻¹]
R_t	L_t/E_d	[sr ⁻¹]
R_w	L_w/E_d	[sr ⁻¹]
ρ_p	L_{pr}/L_d	
$\rho_{p,RS}$	L_{pr}/E_d	[sr ⁻¹]
ρ_{pw}	fraction of L_{ws} reflected by plastic	
ρ_w	L_{wr}/L_d	
$\rho_{w,RS}$	L_{wr}/E_d	[sr ⁻¹]
r_{ws}	L_{ws}/L_{ds}	
τ_p	L_{pt}/L_{ws}	
τ_{pw}	fraction of L_d transmitted through plastic	
τ_w	$L_{ds,0}/L_d$	

3 *)In nadir view

4 back upwards and passes through the water-air interface contains information about the optically
 5 active water constituents. The sub surface irradiance reflectance is generally found to be
 6 proportional to $b_b/(b_b + a)$ (Gordon *et al.*, 1975) or b_b/a (Morel and Prieur, 1977; Kirk, 1991) with
 7 b_b total backscattering coefficient and a total absorption coefficient. The main backscattering
 8 components are suspended sediments and phytoplankton (scattering by water molecules is

1 negligible in comparison). Absorbing components are suspended sediments, phytoplankton,
2 dissolved organic matter, and water itself. The optically active components determine the
3 apparent colour of the water and their concentrations can be estimated from spectral reflectance
4 measurements.

5 Downwelling sunlight consists of direct sunlight (the solar beam) and diffuse sky light (scattered in
6 all directions); the composition of direct and diffuse light depends on the solar elevation angle and
7 sky conditions (Jerlov, 1968). Direct and diffuse skylight interact differently with the water body.

8 **2.2 Light reflectance of water littered with floating plastic**

9 Plastic objects floating on the water surface control surface leaving light in a number of ways, (1)
10 downwelling light reflects differently off plastic than off water, (2) transmittance of downwelling
11 light through plastic is different from transmittance through the air-water interface, changing the
12 underwater light climate and hence the back scattered upwelling light, and (3) subsurface
13 upwelling light transmits through plastic differently than through the water-air interface. The
14 different pathways, illustrated in Fig. 1b, explain why measuring marine plastic is different from
15 retrieving concentrations of optically active water components through their spectral scattering
16 and absorption properties (section 2.1). The mathematical model will have to include radiative
17 transfer in water itself, as well as light interaction with plastics on the water surface with different
18 optical properties (e.g., colour, transparency, and shape). We propose a mathematical model that
19 can help select optimal wavelengths, design experiments, and develop a working algorithm for
20 remote sensing marine plastic.

21 With A_t the total water surface area- and A_p the plastic covered area *projected in nadir view* (Fig.
22 2), the plastic area fraction, f , is defined by A_p/A_t . Both plastic- and open water leaving radiance,

1 L_p and L_w [$\text{Wm}^{-2}\text{sr}^{-1}$], contribute to total above surface upwelling radiance, L_t , leaving this area in
 2 nadir view. L_t received by the sensor in nadir view can be estimated with Eq. (1),

$$3 \quad L_t(\lambda) = (1-f)L_w(\lambda) + fL_p(\lambda) \quad (1)$$

4 For (semi-)transparent plastic, L_p does not only represent plastic reflected sunlight in air, as
 5 subsurface upwelling light that is transmitted through the plastic also contributes to L_p :

$$6 \quad L_p = \rho_p L_d + \tau_p L_{ws} \quad (2)$$

7 Radiance reflectance, ρ_p , is defined as L_{pr}/L_d and transmittance τ_p as L_{pt}/L_{ws} . For a flat horizontal
 8 surface of one single layer of plastic, ρ_p , equals the Fresnel reflectance for normal incident light. In
 9 reality L_p is determined by the object's shape, solidness and surface roughness (through ρ_p) in
 10 combination with the angle of incident light that is reflected in nadir view (L_d) since the angular
 11 distribution of L_d is not uniform. Downwelling sunlight consists of the solar beam and diffuse sky
 12 light, whose proportions depend on sky conditions (e.g., cloudy, clear or hazy), solar elevation angle
 13 and wavelength (Jerlov, 1968). Normal incident light can be regarded as diffuse as the sun is normally
 14 not at zenith angle. We discuss these bi-directional effects and other approximations later in section
 15 3.

16 Subsurface upwelling light, L_{ws} , that is not reflected at the water-plastic interface is transmitted
 17 through the plastic object where light may be lost due to absorption and internal reflection. We
 18 define τ_p as the fraction of subsurface upwelling light hitting the plastic object that was not lost. Eqs.
 19 (1) and (2) lead to an estimation of f

$$20 \quad f(\lambda) = \frac{L_t(\lambda) - L_w(\lambda)}{L_p(\lambda) - L_w(\lambda)} = \frac{L_t(\lambda) - L_w(\lambda)}{\rho_p(\lambda)L_d(\lambda) + \tau_p(\lambda)L_{ws}(\lambda) - L_w(\lambda)} \quad (3)$$

1 L_{ws} in water is estimated from L_w in air by accounting for the loss caused by internal reflection, ρ_0 , at
 2 the water-air interface and the effect of the radiant flux being confined to a wider solid angle of light
 3 as it passes across the water-air interface. According to Austin (1980), radiance increases with a
 4 factor 1.84 as it transfers from air to seawater. L_w is the sum of water surface reflected sunlight, L_{wr} ,
 5 and subsurface upwelling light transmitted through the water surface, L_{wt} (Fig. 1); knowing this, we
 6 can write L_{ws} in above surface terms,

$$7 \quad L_{ws} = 1.84L_{wt} = 1.84(L_w - \rho_w L_d) \quad (4)$$

8 with ρ_w the direct reflectance of seawater from air to seawater similar to the Fresnel reflectance of
 9 seawater for 0° angle of incidence (Hobson & Williams, 1971). In pure water the wavelength
 10 dependence of ρ_w is negligible for wavelengths between 400 to 2000 nm with refractive index
 11 decreasing from 1.343 to 1.304 (Irvine & Pollack, 1968). Thus 2.1% to 1.7% of the light incident
 12 normally on the air-water interface will be reflected back at these wavelengths (Hecht & Zajac, 1974).

13 Using Eq. (4), we can express Eq. (3) solely in terms of radiance measurements in air,

$$14 \quad f(\lambda) = \frac{L_t(\lambda) - L_w(\lambda)}{\rho_p(\lambda)L_d(\lambda) + \tau_p(\lambda)1.84[L_w(\lambda) - \rho_w L_d(\lambda)] - L_w(\lambda)} \quad (5)$$

15 A common definition of reflectance in remote sensing is the ratio of upwelling light, L , and total
 16 downwelling irradiance, E_d [Wm^{-2}],

$$17 \quad R(\lambda) = L(\lambda)/E_d(\lambda) [sr^{-1}] \quad (6)$$

18 We compute R for nadir-viewing directions but in actual airborne or satellite remote sensing the
 19 sensor usually observes in an off-nadir direction. The correction for this is beyond the scope of this

1 paper. Using R_i with subscript “ i ” relating to L_i (Table 1), $\rho_{p,RS} = L_{pr}/E_d$ and $\rho_{w,RS} = L_{wr}/E_d$, Eqs. (3) & (5)
 2 can be written as

$$3 \quad f(\lambda) = \frac{R_t(\lambda) - R_w(\lambda)}{R_p(\lambda) - R_w(\lambda)} = \frac{R_t(\lambda) - R_w(\lambda)}{\rho_{p,RS}(\lambda) + \tau_p(\lambda)1.84(R_w(\lambda) - \rho_{w,RS}) - R_w(\lambda)} \quad (7)$$

4 Eq. (7) shows how the plastic fraction can be estimated from RS measurements in air if $\rho_{p,RS}$, τ_p and
 5 $\rho_{w,RS}$ are known. L_w , and hence R_w , is not strictly the same in open waters as in plastic littered waters
 6 because the presence of floating plastic can affect underwater light climate through shading and
 7 filtering. Therefore, using $R_{w,0}$ to estimate R_w is an approximation:

$$8 \quad f(\lambda) = \frac{R_t(\lambda) - R_{w,0}(\lambda)}{\rho_{p,RS}(\lambda) + \tau_p(\lambda)1.84(R_{w,0}(\lambda) - \rho_{w,RS}) - R_{w,0}(\lambda)} \quad (8)$$

9 In the next section (section 3.3) we evaluate this approximation. This single band algorithm is
 10 expected to work best for wavelengths where $R_{w,0}$ is near zero but where R_p is high, for example a
 11 wavelength of 750 nm (spectra from Asner, 2016). When using larger wavelengths in the SWIR, note
 12 that pure water has absorption peaks near 1.45 μm , 1.94 μm and 2.95 μm (Irvine & Pollack, 1968).
 13 Absorption at the latter wavelength is $11.7 \times 10^{-6} \text{ m}^{-1}$, indicating that a thin film of water on the
 14 plastic can significantly reduce plastic leaving light.

15 The inverse of the derivative of Eq. (8) with respect to R_t computes the sensitivity of R_t to changes
 16 in f ,

$$17 \quad dR_t(\lambda)/df = \rho_{p,RS}(\lambda) + \tau_p(\lambda)1.84(R_{w,0}(\lambda) - \rho_{w,RS}) - R_{w,0}(\lambda) \quad (9)$$

18 We calculated $dR_t(850)/df$ for a single solid flat layer of plastic so that L_d represents light of normal
 19 incidence for light reflected in nadir view. L_d is composed of diffuse sky light if the sun is not in

1 zenith, and if we that assume that sky radiance is completely diffuse, downwelling diffuse
 2 irradiance, $E_{d,dif}$, equals πL_d (Jerlov, 1968). Dekker (1990) measured diffuse irradiance fractions, F
 3 defined by $E_{d,dif}/E_d$, under various cloudless sky conditions. F decreases with increasing
 4 wavelength, and for 850 nm wavelength he found F to be 0.07(0.23) for a clear (hazy) sky. Using
 5 this, $E_d = E_{d,dif}/F$, so that $\rho_{p,RS} = \rho_p/(\pi/F)$ and $\rho_{w,RS} = 0.02/(\pi/F)$. Plastic reflectance in nadir direction,
 6 and hence dR_t/df , therefore increases with increasing fraction of diffuse sky light. In the NIR,
 7 subsurface RS reflectance is less than 1% for wavelengths for most natural water types but higher
 8 for turbid waters where it is 1-2% (Moore *et al.*, 2014). The term ($R_{w,0} - \rho_{w,RS}$) in Eqs. (7)-(9) is
 9 therefore dominated by $R_{w,0}$. We evaluated Eq. (9) for ρ_p and τ_p ranging from 0 to 1; for light hitting
 10 the plastic at zero incidence, transmittance of upwelling light is the same as for downwelling light
 11 and $\rho_p + \tau_p + \alpha_p = 1$, with α_p the light absorbed in the plastic. We repeated this for subsurface RS
 12 reflectance of 0.005, 0.01, 0.02 and 0.035, corresponding with $R_{w,0}$, levels of 0.003, 0.005, 0.01,
 13 0.02 respectively according to the standard NASA conversion from above-water to below-water
 14 (Moore *et al.*, 2014). We did this for F of 0.07 and of 0.23 to examine the effect of lighting
 15 conditions. The results (Fig. 3) confirm that the RS signal is expected to increase with decreasing
 16 $R_{w,0}$ and with increasing F . If $R_{w,0}$ is small, the signal is controlled by plastic reflectance and increasing
 17 with increasing ρ_p . This can be explained as for increasing $R_{w,0}$, reflectance is no longer uniquely
 18 important, with the signal increasing / decreasing with increasing transparency / absorption.
 19 For high $R_{w,0}$, dR_t/df can become zero and then negative indicating that the RS signal reduces with
 20 increasing plastic fraction. Eq. (8) will therefore perform better in clearer waters.

21 **Dual band algorithm**

1 Effects of the varying background colour of natural water should be taken into account and a
 2 possibility is measuring spectral reflectance at more than one wavelength to separate the plastic-
 3 from the water signal. If we can find a second wavelength for which $R_w(\lambda_1) \approx R_w(\lambda_2)$ and $R_p(\lambda_1) \neq$
 4 $R_p(\lambda_2)$ then we can estimate f with:

$$5 \quad f(\lambda_1, \lambda_2) = \frac{R_t(\lambda_1) - R_t(\lambda_2)}{R_p(\lambda_1) - R_p(\lambda_2)} \quad (10a)$$

$$6 \quad f(\lambda_1, \lambda_2) = \frac{R_t(\lambda_1) - R_t(\lambda_2)}{\rho_{p,RS}(\lambda_1) - \rho_{p,RS}(\lambda_2) + 1.84(\tau_p(\lambda_1) - \tau_p(\lambda_2))(R_w(\lambda_1) - \rho_{w,RS}(\lambda_1))} \quad (10b)$$

7 A possibility could be a λ_1 in the VIS-NIR and a second higher wavelength, λ_2 , in the SWIR (spectra
 8 from Asner, 2016).

9 **3 DISCUSSION**

10 **3.1 Approximations**

11 For the derivation of our model, a number of approximations were necessary. First, the proposed
 12 reflectance model is for one type of plastic in two dimensions, i.e., a single smooth flat layer with
 13 specific physical and optical properties, while in reality marine plastic litter consists of all kinds of
 14 shapes and chemical compositions. In truth, a plastic litter object is three dimensional and could
 15 reflect light back in the sensor's view from its sides, especially when it is pitching and rolling on the
 16 ocean waves. Also, if three dimensional shapes change the lighting environment near the sea
 17 surface, they can affect each other's light reflectance. In these cases, plastic reflectance is also
 18 dependent on plastic concentration and $\rho_{p,RS}(\lambda) = \rho_{p,RS}(\lambda, f)$. A plastic surface is usually not just a
 19 specular reflector as illustrated in Fig. 1b (smooth surface), but can reflect light in more than one
 20 direction as well (rough surface). The latter is known as diffuse reflection and enhances $\rho_{p,RS}$ because

1 not only sky light is scattered in nadir view, the solar beam is as well. (The enhancement is
2 comparable to the one by the fraction diffuse sky light as described in section 2.2). To complicate
3 things further, if the plastic surface is wet, water can fill in the gaps and smooth out the surface
4 thereby reducing diffuse reflectance. In addition, water absorbs strongly in at wavelengths in the
5 infrared and a thin layer of water can reduce the signal further at these wavelengths.

6
7 A next step will be to investigate further how dissimilar the different plastics interact with light at
8 the wavelengths of interest and how their signals can be 'mixed'. For a mix of a number of m plastic
9 litter types ' i ' in the water, each with $\rho_{p,RS,i}(\lambda)$ and fraction f_i (total $f = \sum f_i$), a first approximation of
10 their combined signal could be

$$11 \quad R_t(\lambda) = R_{w,0}(\lambda) + \sum_{i=1}^m f_i \rho_{p,RS,i}(\lambda, f_1, \dots, f_m) - R_{w,0}(\lambda) \quad (11)$$

12 The challenge of Eq. (11) is, is to invert it and derive f_i and total f from R_t ; in theory we could apply
13 different wavelengths, selected from the plastic reflectance spectra, to reveal different plastic
14 fractions. The idea is that by selecting the wavelength of an absorption band of a plastic type, this
15 plastic would be excluded from the signal.

16
17 Marine plastic litter that has spent some time in the ocean usually does not have a clean surface but
18 is fouled by a variety of marine life. Organisms such as barnacles or seaweeds growing on the plastic
19 can sink a plastic object below the water surface, hiding it from view. A biofilm of algae reduces
20 reflectance of visible light by light absorption. Different species of algae contain different pigments
21 with unique absorption bands, but all algae contain chlorophyll which absorbs around 672 – 680 nm.
22 All macro- and microalgae have low reflectance in the visible and high reflectance in the NIR. For our

1 RS algorithm we should therefore select wavelength(s) in the infrared rather than in the visible
2 spectrum. How biofilms affect the optical properties of the plastic they inhabit is a subject of future
3 study, using marine plastic litter collected at sea or on the beach.

4
5 In theory our method of geometrical optics applies to objects whose dimensions are larger than a
6 couple of radiance wavelengths (in the order of micrometres in the VIS-SWIR spectrum) and would
7 therefore include microplastics but particles this small are quickly removed from the ocean surface
8 (Eriksen *et al.*, 2014). For particles small in comparison to the wavelength, light scattering is known
9 as Rayleigh scattering (Hecht & Zajac, 1974). Because we only consider surface plastic, studies of the
10 composition of marine plastic and their vertical profiles are necessary to get a full picture of marine
11 plastic pollution. Plastic pollution can be problem in freshwater as well (Driedger *et al.*, 2015) and
12 our suggested RS algorithm could apply here too but it will not work as well in turbid waters due to
13 the higher subsurface reflectance in the NIR (Moore *et al.*, 2014). Also freshwaters are more likely
14 to have emerging vegetation interfering with the RS signal. Oceans are generally clearer than coastal
15 and inland water, and we expect our model to perform better in the open ocean. Other
16 approximations are the bi-directionality of the plastic reflectance of sunlight and the shading and
17 filtering of downwelling light by plastic on the water surface. These issues will be discussed in the
18 following.

19 **3.2 Bidirectional reflectance of marine plastic litter**

20 RS algorithms linking a water body's inherent optical properties to reflectance values are based on
21 subsurface irradiance reflectance or reflectance defined by the ratio of subsurface upwelling
22 radiance and above surface downwelling irradiance. The water body below the surface is

1 sometimes treated as a Lambertian reflector (reflected light is completely diffuse and unpolarised
2 so that $E_{ws}/L_{ws} = \pi$, (Jerlov, 1968) independent on the angle of incidence. This assumption cannot
3 be made for plastic objects as the reflectance of plastic objects, ρ_p , is dependent on the angle of
4 the light of incidence. We assumed 0° angle of incident radiance, θ_i , (section 2.2), which corresponds
5 with a flat plastic surface at right angles with incoming radiance. In reality, plastic litter can have
6 many shapes with surfaces at different angles, and downwelling radiance at different angles is
7 reflected in nadir direction $L_{pr} = L_d(\theta_i)\rho_p(\theta_i)$. However, marine plastics floating on the sea surface
8 pitch and roll on the waves, producing more equally distributed reflected light. In addition,
9 downwelling light is not completely diffuse so that $\rho_{p,RS}$ is also dependent on the angular distribution
10 of downwelling light ($\rho_{p,RS} = \rho_p(\theta_i)L_d(\theta_i)/E_d$). The angular distribution depends on the composition of
11 sunlight of direct light and diffuse skylight, controlled by the solar elevation angle and sky conditions
12 such as cloud cover (Jerlov, 1968). How this averages out depends on the integration time of the
13 recorded light. If A_t is not small compared to the distance between the sea surface and the sensor,
14 the position of A_p within can also modify the measured radiance, i.e., plastic objects in the centre
15 will contribute more than those nearer the edge. As floating objects move around on the sea
16 surface, this may also average out in practice.

17 **3.3 Shading and filtering of downwelling light by plastic**

18 Sub-surface upwelling radiance, L_{ws} , changes in the presence of surface plastic because of changes
19 in sub-surface downwelling radiance, L_{ds} , ($L_{ws} = r_{ws}L_{ds}$ and $L_{ws,0} = r_{ws}L_{ds,0}$). However, subsurface
20 radiance reflectance in the water body below the surface should be the same with and without
21 plastic coverage ($r_{ws} = L_{ws,0}/L_{ds,0} = L_{ws}/L_{ds}$). Assume L_{ds} is a fraction of $L_{ds,0}$ by a spectral shading
22 factor, ε , depending on how much plastic is covering the water surface ($L_{ds} = \varepsilon(f,\lambda)L_{ds,0}$, and hence

1 $L_{ws} = \varepsilon(f, \lambda)L_{ws,0}$, with $\varepsilon(f=0) = 1$ and $\varepsilon(f > 0) < 1$). Using Eq. (4), $L_{w,0} = L_{ws,0}/1.84 + \rho_w L_d$ and
 2 $L_w = L_{ws}/1.84 + \rho_w L_d$, leads to

$$3 \quad L_w = \varepsilon L_{w,0} + \rho_w (1 - \varepsilon) L_d \Rightarrow R_w = \varepsilon R_{w,0} + \rho_{w,RS} (1 - \varepsilon) \quad (12)$$

4 With Eq. (12) and $L_{ws} = \varepsilon(f, \lambda)L_{ws,0}$, Eq. (7) can be rewritten in terms of in air measurements of total
 5 RS reflectance and RS reflectance of the open water surface,

$$6 \quad f(\lambda) = \frac{R_t(\lambda) - [\varepsilon(f, \lambda)R_{w,0}(\lambda) + \rho_{w,RS}(1 - \varepsilon(f, \lambda))]}{\rho_{p,RS}(\lambda) + \tau_p(\lambda)\varepsilon(f, \lambda)1.84(R_{w,0}(\lambda) - \rho_{w,RS}) - [\varepsilon(f, \lambda)R_{w,0}(\lambda) + \rho_{w,RS}(1 - \varepsilon(f, \lambda))]} \quad (13)$$

7 If we disregard change in the subsurface radiance caused by plastic floating at the surface, i.e., $\varepsilon \approx$
 8 1, Eq. (13) reduces to Eq. (8). We can solve Eq. (13) with an iterative calculation using the
 9 relationship between $\varepsilon(f, \lambda)$ and f (Eq. (A3)). In Appendix A1 a theoretical equation for the spectral
 10 shading factor is derived from the optical model.

11 **3.4 Future work**

12 Field

13 In the proposed field experiment, a range of plastic fractions of one similar, common type (e.g.,
 14 plastic drink bottles or carrier bags) on a restricted area of sea surface is placed in the field of view
 15 (Fig. 2) and L_t and E_d are measured using a spectrometer in the VIS-SWIR spectrum. $L_{w,0}$, is
 16 measured using the same system but in the absence of plastic. By controlling the field of view of
 17 the radiometer, a sufficiently large and constant sea surface is measured. Thus values of $R_{w,0}(\lambda)$
 18 and of $R_t(\lambda)$ are measured as a function of f . A linear fit to Eq. (8) for $R_{w,0} \approx \rho_{w,RS}$, rewritten as Eq.
 19 (14), of the measurements can give $\rho_{p,RS}(\lambda)$:

$$R_t(\lambda) = R_{w,0}(\lambda) + f(\rho_{p,RS}(\lambda) - R_{w,0}(\lambda)) \quad (14)$$

If we consider the shading, Eq. (13) can be similarly rewritten, with $\rho_{w,RS} \approx 0$,

$$R_t(\lambda) = \varepsilon(f, \lambda)R_{w,0}(\lambda) + f(\rho_{p,RS}(\lambda) - \varepsilon(f, \lambda)R_{w,0}(\lambda)) \quad (15)$$

The theoretical equation for $\varepsilon(f, \lambda)$ can be expressed as $(1 - c_1f)/(1 - c_2f)$ (Eq. (A3)), so if we have enough measurements of R_t over a range of f values we could find c_1 , c_2 (and thus ε), and $\rho_{p,RS}(\lambda)$ through curve fitting. It would be possible to examine the magnitude of $\varepsilon(f, \lambda)$ from measurements of $L_{ds}/L_{ds,0}$ for the range of f values, using an underwater spectroradiometer (e.g., Potes *et al.*, 2013). Experimentally derived $\varepsilon(f, \lambda)$ and $\rho_{p,RS}(\lambda)$ represent the plastic objects shape and not just apply for a single flat layer of plastic. The sample site should be clear water as in turbid waters it will be harder to see a plastic signal (section 2.2).

Laboratory

Reflectance and transmittance of the plastic measured in the laboratory (in a benchtop spectrometer, using the spectrometer with a contact probe, or using the spectrometer with a stable and calibrated light source) are not the same as, but related to τ_p and $\rho_{p,RS}$ respectively. The relation between $\rho_{p,RS}$ (τ_p) derived from the field observations and measured reflectance (transmittance) can clarify how the shape of a plastic object and the composition of natural daylight affect $\rho_{p,RS}$ (τ_p) The laboratory measurements will help select wavelengths for which plastic reflectance is high and -transmittance low and will add to the spectral library of the spectrum characteristic of plastic debris types, which will be very valuable to the marine plastics science community (Maximenko *et al.*, 2016).

1 Satellite remote sensing

2 Emberton *et al.* (2015) give an overview of satellite based multispectral and hyperspectral ocean
3 colour remote sensors of the past, present and future. Satellites that carry ocean colour sensors
4 usually carry other instruments that are useful for marine plastic detection. For example the OLCI
5 ocean colour instrument with 21 bands in the VIS-NIR (0.4-1.02 μm) on Sentinel-3 works in synergy
6 with Sentinel-3's SLSTR instrument comprising nine bands in the VIS-SWIR 0.55-12 μm (ESA, 2017).
7 It will be interesting to see if satellite measurements in the spectral bands of our choice applied to
8 our reflectance model can replicate the global distribution of marine plastics calculated by various
9 particle-tracking models (e.g., van Sebille *et al.*, 2012; 2015) and ocean surveys (Eriksen *et al.*,
10 2014; C3zar *et al.*, 2017). Of special interest are the "hot spots" of marine plastics such as the
11 centres of the subtropical gyres predicted by these models but never seen from space before. The
12 biggest hotspot of all is located in the North Pacific between Hawai'i and California (Law *et al.*,
13 2014). Hard to reach areas, such as the Arctic, could really benefit from RS observations. Floating
14 plastic accumulation is predicted in the Arctic (van Sebille *et al.*, 2012) but this region of the ocean
15 is difficult to survey extensively (C3zar *et al.*, 2017). However, the most common atmospheric
16 correction method is the black pixel approach, which assumes that water-leaving radiance, L_{wt} , is
17 equal to zero in the NIR or SWIR so that the measurements taken from a band in one of these
18 regions only contain aerosol atmospheric and ocean surface effects. This correction would
19 therefore likely conceal the signal in the NIR and SWIR from plastic in the ocean and we would
20 need the uncorrected data. An alternative atmospheric and sun glint correction algorithm,
21 POLYMER, derives ocean colour parameters in the whole sun glint spectrum and does not require
22 negligible water reflectance in near infrared bands (Steinmetz *et al.*, 2011). POLYMER is based on
23 a model, extended from 700 nm to 900 nm by using the similarity spectrum for turbid waters

1 (Ruddick *et al.*, 2006), which may remove optical signal from sea surface plastic. Oceanic whitecaps
2 are reflective in the solar spectral range (Koepke, 1984) and therefore capable of corrupting the
3 marine plastic signal. We therefore recommend the use of satellite data for marine plastic
4 estimations under low wind speed conditions; whitecapping is negligible when the wind speed is
5 less than 3 or 4 ms^{-1} (Goddijn-Murphy *et al.*, 2011). Wave height and wind over the ocean can be
6 estimated from radar altimetry, for example the SRAL altimeter on board Sentinel-3 (ESA, 2017).

7 **4 CONCLUSION**

8 We have presented an optical reflectance model that can be used as a first step towards a remote
9 sensing algorithm for marine plastic litter. There are many types of marine plastic litter and we have
10 considered floating macroplastics of one type for simplicity. If we know RS reflectance of the clear
11 sea surface, $R_{w,0}(\lambda)$, and of the plastic, $\rho_{p,RS}(\lambda)$, we can estimate the fraction of plastic surface area
12 from measurements in air. We can approximate $R_{w,0}(\lambda)$ if the water type is known (e.g., Moore *et al.*,
13 2014; Mélin & Vantrepotte, 2015), and derive $\rho_{p,RS}(\lambda)$ from the proposed field measurements, or
14 they could be used as tuning parameters. It may be necessary to account for shading of surface
15 plastic, i.e., reduced subsurface light due surface plastic blocking downwelling sunlight. Key is to
16 select a wavelength for which water leaving light is minor and plastic reflectance is high, for example
17 around 750 nm, (single band algorithm), or two wavelengths for which water reflectance is near
18 equal and the reflectance of the plastic is not (dual band algorithm).

19

20 *Acknowledgements*

21 This work was made possible by the Carnegie Trust, Research Incentive Grant (70649). In addition,
22 the ERDF Interreg VB Northern Periphery and Arctic (NPA) Programme funded this activity through

- 1 the Circular Ocean project. Erik van Sebille was supported through funding from the European
- 2 Research Council (ERC) under the European Union's Horizon 2020 research and innovation
- 3 programme (grant agreement No 715386).

1 APPENDIX

2 *A1. Computation of the spectral shading factor*

3 The relationship between ε and f can be predicted using the same optical model as for modelling
4 light reflectance in air (section 2.2). The expression corresponding to Eq. (1) is,

5
$$L_{ds}(\lambda) = (1-f)L_{ds,0}(\lambda) + fL_{ps}(\lambda) \quad (\text{A1})$$

6 with L_{ps} subsurface downwelling plastic leaving radiance. In analogy with Eq. (2), we describe L_{ps}
7 as,

8
$$L_{ps} = \tau_{pw}L_d + \rho_{pw}L_{ws} \quad (\text{A2})$$

9 with τ_{pw} the fraction of downwelling light in air transmitted through the plastic object into the water,
10 and ρ_{pw} the subsurface reflectance at the water-plastic interface (respectively independent and
11 dependent on the sun angle). Using $\varepsilon(f,\lambda) = L_{ds}/L_{ds,0} = L_{ws}/L_{ws,0}$, $L_{ws} = r_{ws}L_{ds}$, and $\tau_w = L_d/L_{ds,0}$, it can
12 be shown that

13
$$\varepsilon(f, \lambda) = \frac{1 - f(1 - \tau_{pw}(\lambda) / \tau_w(\lambda))}{1 - f\rho_{pw}r_{ws}} \quad (\text{A3})$$

14

1 REFERENCES

- 2 Andrady, A. L., Neal, M.A., 2009. Applications and societal benefits of plastics. Philosophical
3 transactions of the Royal Society of London. Series B, Biological sciences, 364, 1977–1984.
- 4 Andrady, A. L., 2015. Persistence of Plastic Litter in the Oceans, in: Bergmann, M., Gutow, L.,
5 Klages, M. (eds), Marine Anthropogenic Litter, Springer Open, Springer International Publishing AG
6 Switzerland. doi: 10.1007/978-3-319-16510-3.
- 7 Asner, 2016. Workshop on Mission Concepts for Marine Debris Sensing, January 19-21, 2016, East-
8 West Center of the University of Hawaii at Manoa, Honolulu, Hawaii, available online:
9 http://iprc.soest.hawaii.edu/NASA_WS_MD2016/pdf/Asner2016.pdf (accessed on 9 August 2017).
- 10 Austin, R. W., 1980. Coastal Zone Color Scanner Radiometry, Proc. SPIE 0208, Ocean Optics VI, 170
11 (March 26, 1980). doi:10.1117/12.958273.
- 12 Cózar, A., Martí, E., Duarte, C. M., García-de-Lomas, J., van Sebille, E., Ballatore, T. J., *et al.*, 2017.
13 The Arctic Ocean as a dead end for floating plastics in the North Atlantic branch of the
14 Thermohaline Circulation, Science Advances, 3: e1600582.
15 <http://advances.sciencemag.org/cgi/content/full/3/4/e1600582/DC1>
- 16 Dekker, A. G., 1990. Detection of optical water quality parameters for eutrophic waters by high
17 resolution remote sensing. PhD Thesis, Vrije Universiteit, Amsterdam.
- 18 Dobretsov S., Thomason, J. C., Williams, D. N., 2014. Biofouling methods, West Sussex, England,
19 John Wiley & Sons, Ltd.

1 Driedger, A. G. J., Dürr, H. H., Mitchell, K., Van Cappellen, P., 2015. Plastic debris in the
2 Laurentian Great Lakes: A review. *Journal of Great Lakes Research*, Volume 41, Issue 1, Pages 9-
3 19. doi:10.1016/j.jglr.2014.12.020.

4 Emberton, S., Chittka, L., Cavallaro, A., Wang, M., 2016. Sensor Capability and Atmospheric
5 Correction in Ocean Colour Remote Sensing. *Remote Sensing*, 8, 1. doi:10.3390/rs8010001.

6 Eriksen M., Lebreton, L. C. M., Carson, H., S., Thiel, M., Moore, C. J., Borerro, J. C., Galgani, F., Ryan,
7 P. G., Reisser, J., 2014. Plastic Pollution in the World's Oceans: More than 5 Trillion Plastic Pieces
8 Weighing over 250,000 Tons Afloat at Sea. *PLoS ONE* 9(12): e111913.
9 doi:10.1371/journal.pone.0111913.

10 ESA, 2017. Sentinel Online, User Guides, available online:
11 <https://sentinel.esa.int/web/sentinel/user-guides/> (accessed on 9 August 2017).

12 Filella, M., 2015. Questions of size and numbers in environmental research on microplastics:
13 methodological and conceptual aspects. *Environmental Chemistry*, 12(5), 527-538.
14 doi:10.1071/EN15012.

15 Goddijn-Murphy, L., D. K. Woolf, and A. H. Callaghan, 2011. Parameterizations and algorithms for
16 oceanic whitecap coverage. *Journal of Physical Oceanography*, 41(4), 742-756. doi:
17 10.1175/2010JPO4533.1.

18 Gordon, H.R., O.B. Brown, O.B., Jacobs, M. M., 1975. Computed relationships between the
19 inherent and apparent optical properties of a flat homogeneous ocean. *Applied Optics*, 14, 417-
20 427.

- 1 Gregory, M. R., 2009. Environmental implications of plastic debris in marine settings—
2 entanglement, ingestion, smothering, hangers-on, hitch-hiking and alien invasions. *Philosophical*
3 *transactions of the Royal Society of London. Series B, Biological sciences*, 364(1526), 2013–2025.
4 doi:10.1098/rstb.2008.0265.
- 5 Hecht, E., Zajac, A., 1974. *Optics*, Addison-Wesley Publishing Company, Inc., Massachusetts.
- 6 Irvine, W. M. J.B., Pollack, J. B., 1968. *Infrared Optical Properties of Water and Ice Spheres*, Icarus
7 Vol. 8.
- 8 Hobson, D. E., Williams, D., 1971. Infrared Spectral Reflectance of Sea Water, *Applied Optics*, 10,
9 2372-2373. doi: 10.1364/AO.10.002372.
- 10 Jambeck, J.R., Geyer, R., Wilcox, C, Siegler, T. R., Perryman, M., Andrady, A., *et al.*, 2015. Plastic
11 waste inputs from land into the ocean. *Science*, 347 (6223), 768–771.
- 12 Jerlov, N. G., 1968. *Optical oceanography*. Amsterdam, Elsevier publishing company.
- 13 Kirk, J. T. O., 1994. *Light & photosynthesis in aquatic ecosystems*. Cambridge, Cambridge University
14 Press.
- 15 Koepke, P., 1984. Effective reflectance of oceanic whitecaps. *Applied Optics*, Vol. 23, No. 11.
- 16 Laist D.W., 1997. Impacts of Marine Debris: Entanglement of Marine Life in Marine Debris Including
17 a Comprehensive List of Species with Entanglement and Ingestion Records. In: Coe J.M., Rogers
18 D.B. (eds) *Marine Debris*. Springer Series on Environmental Management. Springer, New York, NY
- 19 Law, K. L., Morét-Ferguson, S. E., Goodwin, D. S., Zettler, E. R., DeForce, E., Kukulka, T.,
20 Proskurowski, G., 2014. Distribution of Surface Plastic Debris in the Eastern Pacific Ocean from an

1 11-Year Data Set. *Environmental Science and Technology*, 48, 4732–4738.
2 doi.org/10.1021/es4053076.

3 Maximenko, N., Arvesen, J., Asner, G., Carlton, J., Castrence, M., Centurioni, L., *et al.*, 2016. Remote
4 sensing of marine debris to study dynamics, balances and trends. Community white paper
5 produced at the Workshop on Mission Concepts for Marine Debris Sensing, January 19-21, 2016,
6 East-West Center of the University of Hawaii at Manoa, Honolulu, Hawaii. Submitted to: Decadal
7 Survey for Earth Science and Applications from Space.

8 Mélin, F., Vantrepotte, V., How optically diverse is the coastal ocean?, 2015. *Remote Sensing of*
9 *Environment*, 160, 235-251. [doi:10.1016/j.rse.2015.01.023](https://doi.org/10.1016/j.rse.2015.01.023).

10 Moore, T. S., Dowell, M. D., Bradt, S., Antonio Ruiz Verdud, A. R., 2014. An optical water type
11 framework for selecting and blending retrievals from bio-optical algorithms in lakes and coastal
12 waters. *Remote Sensing of Environment*, 143, 97–111. [doi:10.1016/j.rse.2013.11.021](https://doi.org/10.1016/j.rse.2013.11.021).

13 Morel, Y. A., Prieur, L., 1977. Analysis of variations in ocean color. *Limnology and Oceanography*
14 22(4): 709-722.

15 Mrosovsky, N., Ryan, G. D., James, M. C., 2009. Leatherback turtles: The menace of plastic. *Marine*
16 *Pollution Bulletin* 58(2) 287:289.

17 Potes, M., João Costa, M., Salgado, R., Bortoloi, D., Serafim, A., Le Moigne, P., 2013. Spectral
18 measurements of underwater downwelling radiance of inland water bodies. *Tellus*, 65, 20774.
19 [doi: 10.3402/tellusa.v65i0.20774](https://doi.org/10.3402/tellusa.v65i0.20774).

1 Rochman, C. M., M. R., Browne, M. A., Underwood, A. J., van Franeker, J. A., Thompson, R. C.,
2 Amaral-Zettler, 2016. The ecological impacts of marine debris: unravelling the demonstrated
3 evidence from what is perceived. *Ecology*, 97(2), 2016, pp. 302–312. doi:10.1890/14-2070.1.

4 Ruddick, K. G., De Cauwer, V., Park, Y. –J, Moore, G., 2006. Seaborne measurements of near
5 infrared water-leaving reflectance: The similarity spectrum for turbid waters. *Limnology and*
6 *Oceanography*, 51(2), 1167–1179. doi:10.4319/lo.2006.51.2.1167.

7 Ryan, P. G., 2015. Does size and buoyancy affect the long-distance transport of floating debris?
8 *Environmental Research Letters*, 10, 084019. doi:10.1088/1748-9326/10/8/084019.

9 Sherman, P., van Sebille, E., 2016. Modeling marine surface microplastic transport to assess
10 optimal removal locations. *Environmental Research Letters*, 11, 014006. doi:10.1088/1748-
11 9326/11/1/014006.

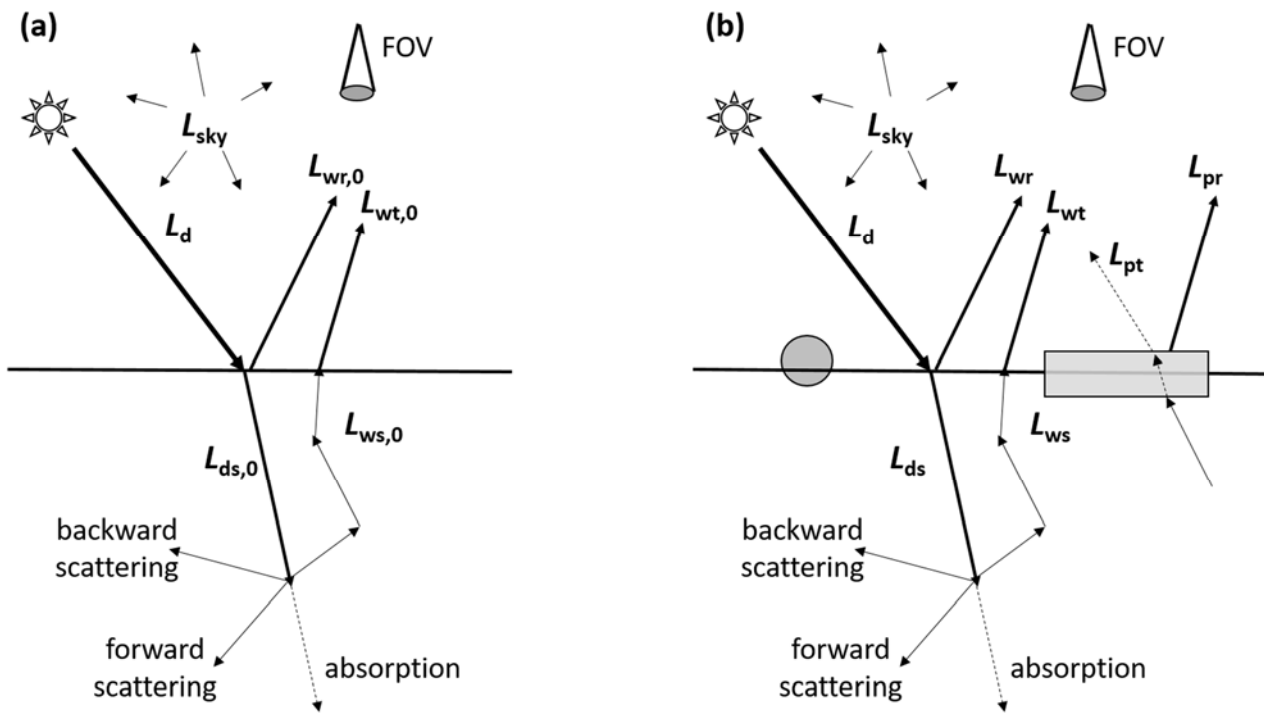
12 Steinmetz, F., Deschamps, P. –Y., and Ramon, D., 2011. Atmospheric correction in presence of sun
13 glint: application to MERIS. *Optical Express*, 19, 9783-9800. doi:10.1364/OE.19.009783.

14 van Sebille, E., C. Wilcox, L. Lebreton, N.A. Maximenko, B.D. Hardesty, J.A. van Franeker, *et al.*,
15 2015. A Global Inventory of Small Floating Plastic Debris. *Environmental Research Letters*, 10 (12),
16 124006. doi:10.1088/1748-9326/10/12/124006.

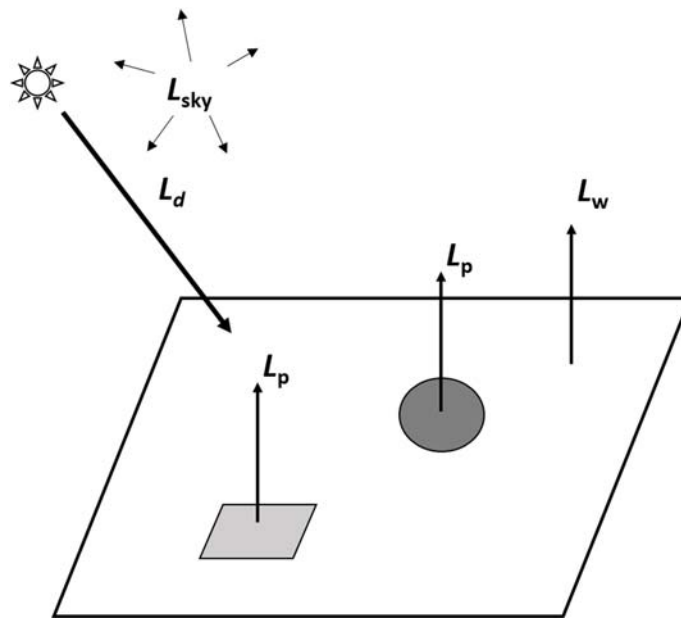
17 van Sebille, E., England, M. H., and Froyland, G., 2012. Origin, dynamics and evolution of ocean
18 garbage patches from observed surface drifters, *Environmental Research Letters*, 7, 044040.
19 doi:10.1088/1748-9326/7/4/044040.

- 1 Wilcox, C, Van Sebille, E., Hardesty, B. D., 2015. Threat of plastic pollution to seabirds is global,
- 2 pervasive, and increasing. PNAS, 112 (38) 11899-11904. doi:10.1073/pnas.1502108112.

1 FIGURES

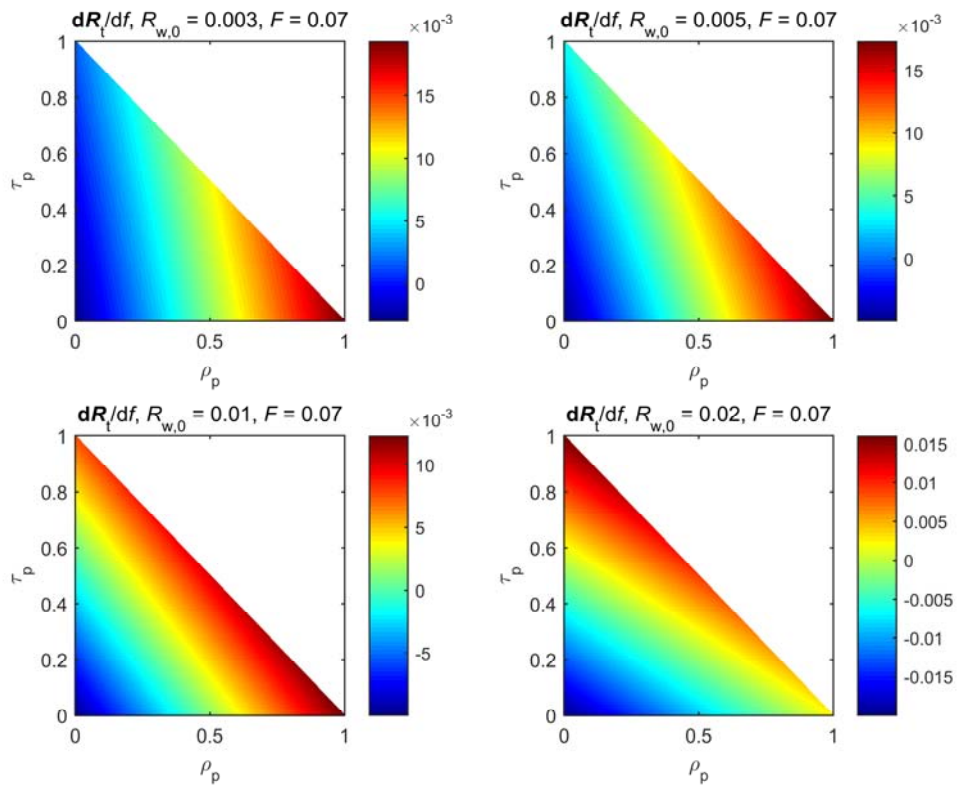


3 *Fig. 1. Schematic of sunlight hitting (a) an open water body, and (b) the same water body with*
 4 *floating plastic. With L_d total downwelling sunlight (solar beam + diffuse sky light), L_{ds} subsurface*
 5 *downwelling light, L_{ws} subsurface upwelling light, L_{wr} light reflected directly off the water surface,*
 6 *L_{wt} subsurface upwelling light transmitted through the water-air interface, L_{pr} light reflected off the*
 7 *plastic and L_{pt} subsurface upwelling light transmitted through the plastic. L_w is total water leaving*
 8 *light, $L_{wr} + L_{wt}$, and L_p is total plastic leaving light, $L_{pt} + L_{pr}$; subscript '0' indicates the variables in the*
 9 *absence of plastic and FOV is field of view.*

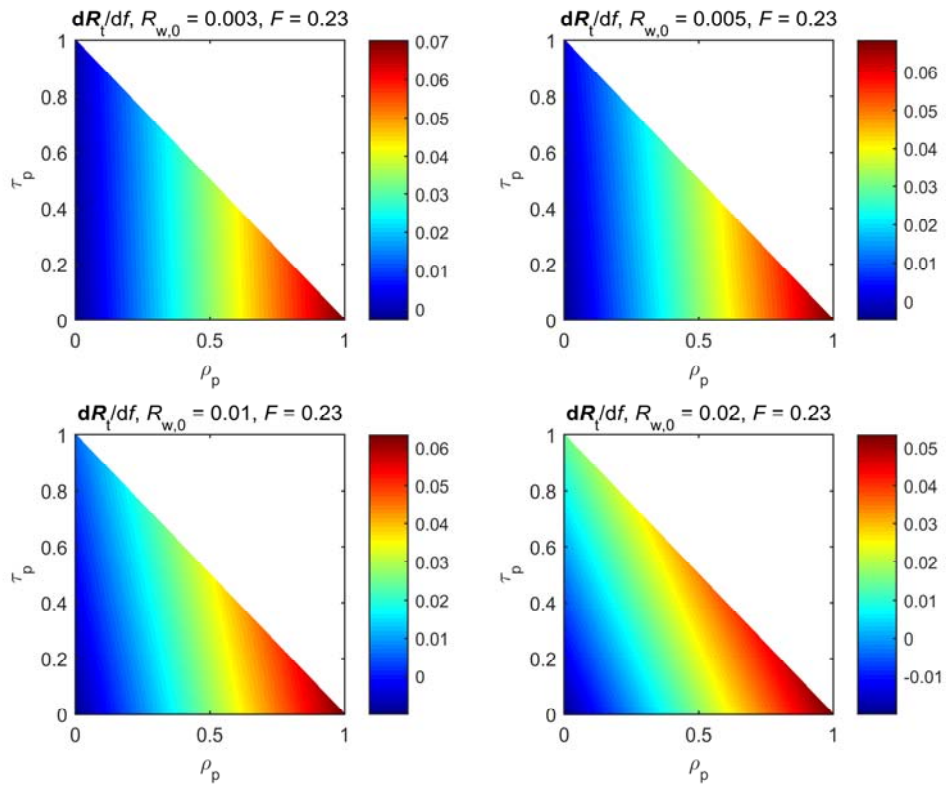


1

2 *Fig. 2. As Fig. 1 but seen from above, with A_t (A_p) total (total plastic) surface area in the frame*
 3 *projected in nadir view, with ρ_p and τ_p (L_{pr}/L_{ws} and L_{pt}/L_{ws} respectively as in Fig. 1b) representing the*
 4 *total spectral radiance reflectance and transmittance of the plastic. The coefficients ρ_p and τ_p are*
 5 *dependent on light conditions, i.e., the solar elevation angle in the field and the fraction diffuse sky*
 6 *light. Eqs. (1) and (2) lead to an estimation of f from remote sensing.*



1



2

1 *Fig. 3. Computations of dR_t/df (Eq. 9) for a flat, single layer piece of plastic with a range of*
2 *reflectance and transmittance coefficients using F at 850 nm wavelength for (top) clear sky ($F =$*
3 *0.07), and (bottom) hazy sky ($F = 0.23$). For $R_{w,0} = 0.003, 0.005, 0.01, \text{ and } 0.02$ (corresponding with*
4 *respective sub surface RS reflectance of 0.005, 0.01, 0.02 and 0.035), for clear to turbid natural*
5 *waters (Moore et al., 2014).*

6